Development 136, 943-953 (2009) doi:10.1242/dev.029363

MIG-32 and SPAT-3A are PRC1 homologs that control neuronal migration in *Caenorhabditis elegans*

Ozgur Karakuzu, David P. Wang and Scott Cameron*

The Polycomb repression complex 2 (PRC2) methylates histone H3 lysine 27 at target genes to modify gene expression, and this mark is recognized by PRC1, which ubiquitylates histone H2A. In *Caenorhabditis elegans*, a complex of the MES-2, MES-3 and MES-6 proteins is functionally analogous to the PRC2 complex, but the functional analog of PRC1, and indeed whether *C. elegans* has such a complex, has been unclear. We describe here that MIG-32 and SPAT-3A are functional analogs of PRC1 in *C. elegans*, where they are required for neuronal migrations and during vulval development. *mig-32* and *spat-3* mutants are defective in H2A ubiquitylation, and have nervous system defects that partially overlap with those of *mes* mutants. However, unlike the *mes* mutants, *mig-32* and *spat-3* mutants are fertile, suggesting that PRC1 function is not absolutely required in the germline for essential functions of PRC2.

KEY WORDS: BMI-1, *C. elegans*, Histone modification, Polycomb, Neuronal migration, ring1B

INTRODUCTION

The Polycomb group genes encode components of chromatin-modifying complexes, and were initially identified in *Drosophila* as modifiers of Hox gene expression that antagonize the action of Trithorax group genes (Kennison and Tamkun, 1988; Lewis, 1978; Nusslein-Volhard et al., 1985; Simon et al., 1992). Biochemical and molecular analyses have defined at least three protein complexes, called Polycomb repressive complex 2 (PRC2), PhoRC and PRC1. PRC2 is a histone methyltransferase that methylates Histone 3 lysine 27, and includes the proteins Enhancer of zeste, Extra sex combs, Su(z)12 and Nurf-55 (Cao et al., 2002; Czermin et al., 2002; Kuzmichev et al., 2002; Muller et al., 2002). The H3K27me3 histone mark is in turn recognized by the PRC1 complex (Cao et al., 2002; Czermin et al., 2002; Kuzmichev et al., 2002; Saurin et al., 2001), which has as core components in human cells Ring1, Ring2/Ring1B, Bmi-1 and HPH2 (Wang et al., 2004a). PRC1 is recruited to sites methylated by PRC2, where the Ring1B protein of PRC1 monoubiquitylates H2A at lysine 119 (Wang et al., 2004a; Wang et al., 2004b). In this complex, BMI-1 enhances the stability and enzymatic activity of Ring1B (Cao et al., 2005). PRC1 inhibits gene expression through mechanisms that are as yet not entirely clear but which may involve repressing the initiation of transcription, inhibiting nucleosome remodeling, regulating association of linker histone H1 and/or chromatin compaction (Francis et al., 2004; King et al., 2002; Levine et al., 2002; Shao et al., 1999; Zhu et al., 2007). Recent genome-wide identification of Polycomb group target genes has also shown that some targets are transcribed despite the presence of Polycomb group proteins on the gene, suggesting that repression may not be a universal outcome at all loci (Boyer et al., 2006; Bracken et al., 2006; Lee et al., 2006; Tolhuis et al., 2006).

Caenorhabditis elegans orthologs of the PRC2 complex have been identified and well characterized. These include the products of the *mes-2*, *mes-3* and *mes-6* genes, mutations in which result in maternal effect sterility (Capowski et al., 1991). The MES proteins form a complex in which the SET domain of MES-2 mediates di- and trimethylation of H3K27 (Bender et al., 2004; Holdeman et al., 1998). The H3K27me3 mark is concentrated on the X chromosome of wild-type animals, and transcription of X chromosome genes is normally silenced in the germline (Fong et al., 2002; Xu et al., 2001b). In *mes-2*, *mes-3* and *mes-6* mutants chromatin marks associated with active chromatin are found on the X chromosome and, according to the current model, inappropriate expression of X chromosome genes in the germline is responsible for the degeneration of germ cells and the sterility observed in *mes* mutants (Fong et al., 2002).

In addition to their role in the germline, *mes* genes also act in somatic cells. *mes-2*, *mes-3* and *mes-6* mutants have weak but reproducible defects consistent with abnormal Hox gene activity, in agreement with the classical role of Polycomb group genes as repressors of Hox gene activity (Ross and Zarkower, 2003). The abnormalities include subtle defects in migration by specific neurons, expansion of the domains of Hox gene expression, and mislocalization of sensory rays in the male tail. The genetic screens that identified the *mes* genes did not identify genes homologous to PRC1 components, and the *C. elegans* genome does not encode obvious homologs of many of the components of PRC1. These data suggest that either *C. elegans* lacks a PRC1 complex, which would suggest that PRC2 function could be uncoupled from PRC1 function, or that the function, composition or amino acid sequences of the proteins in a PRC1-like complex are sufficiently divergent to make recognizing them difficult.

Here we describe the genes *mig-32* and *spat-3*, which encode homologs of the human PRC1 core components Bmi-1 and Ring1B, respectively. Consistent with MIG-32 and SPAT-3 being functionally analogous to PRC1, ubiquitylation of H2A is markedly reduced or absent in *mig-32* and *spat-3* mutants. Both mutants have defects in their nervous system that are similar those of *mes* mutants. Surprisingly, unlike *mes* mutants, *mig-32* and *spat-3* mutants are fertile, suggesting that H2A ubiquitylation by PRC1 is not required in the germline for MES/PRC2 function.

MATERIALS AND METHODS

Alleles and strains

All strains were maintained at 20°C as described by Brenner (Brenner, 1974).

Mutations and mapped integrated transgenes used were as follows. LGI: *mig-1(e1787)*; *mes-3(bn35); unc-73(e936); unc-40(e271); ced-1(e1735)*. LGII: *mes-2(bn11); unc-4(e120); muIs32 [*$P_{mec\text{-}7}$*gfp]* (Pujol et al., 2000);

Departments of Pediatrics and Molecular Biology, Division of Pediatric Hematology-Oncology, University of Texas Southwestern Medical Center at Dallas, Dallas, TX 75390, USA.

*Author for correspondence (e-mail: scott.cameron@utsouthwestern.edu)

Accepted 9 January 2009

muIs16 [P$_{mab-5}$gfp] (Hunter et al., 1999); *nIs128 [P$_{pkd-2}$gfp]* (Yu et al., 2003). LGIII: *pal-1(e2091); mig-10(ct41); unc-119(ed3)*. LGIV: *plx-1(nc37); ced-10(n1993); mes-6(bn38); dpy-20(e1282); mig-32(n4275)* (kindly provided by the Horvitz lab, MIT, Cambridge MA, USA), *mig-32(tm1807), mig-32(tm1684)* (kindly provided by the Mitani lab, Tokyo Women's University, Tokyo, Japan); *unc-31(e928)*. LGV: *him-5(e1490)*. LGX: *nIs106 [P$_{lin-11}$gfp]* (Cameron et al., 2002), *kyIs4 [P$_{ceh-23}$gfp]* (Zallen et al., 1998); *oxIs12 [P$_{unc-47}$gfp]* (McIntire et al., 1997); *unc-6(ev400); mig-2(mu28); slt-1(eh15); lin-15(n765ts); spat-3(gk22)*.

Integrated transgenes not mapped to a chromosome included: *kyIs39 [P$_{sra-6}$gfp]* (Troemel et al., 1995); *bxIs13 [P$_{egl-5}$gfp]* (Zhang and Emmons, 2001); *mxIs23 [P$_{mig-32}$mig-32:gfp]*.

Extra-chromosomal arrays included: *rtEx238 [P$_{nlp-1}$gfp]* (kindly provided by Leon Avery, University of Texas Southwestern Medical Center, Dallas TX, USA); *mxEx53 [P$_{plx-1}$mig-32:cfp]*.

Imaging

Transgenic animals were imaged using a Zeiss Axiophot. To quantitate HSN and ALM migrations, the distance along the body axis between the rectum and the HSN or ALM nuclei was determined using Openlab software and compared to the distance to the vulva.

Construction and analysis of *mig-32/Df* animals

sDf62 unc-31(e169)/nT1(IV); +/nT1(V) hermaphrodites were mated with *him-5(e1490)* males and cross-progeny males were mated with *mig-32(n4275) unc-31(e928)* hermaphrodites. The position of ray-1 in Unc males was determined.

Plasmid constructs and P$_{mig-32}$*mig-32:gfp* construction

To construct P$_{mig-32}$ *mig-32:gfp*, an 8065 bp *Bam*HI/*Sph*I fragment of the F11A10 cosmid was cloned into pUC19. An *Xma*I fragment of pPD102.33, including the GFP coding sequences, was cloned into the *Age*I site in the first exon of *mig-32*. This construct was injected into *lin-15(765ts)* worms, integrated and backcrossed three times to *mig-32(n4275); him-5(e1490)*.

To construct P$_{plx-1}$*mig-32::cfp*, an *Eco*RI-*Xba*I fragment of the full-length yk1321a11 *mig-32* cDNA was cloned into pUC19. CFP coding sequences were amplified by PCR and cloned into *mig-32* at the *Age*I site. The *mig-32* start codon was converted into an *Nsi*I site using site-directed mutagenesis, and 2.6 kb of the *plx-1* promoter (Dalpe et al., 2004) was PCR amplified and cloned into the *Nsi*I site. Constructs were injected into *unc-119(ed3); mig-32(n4275); him-5(e1490)* worms using *unc-119* as the co-injection marker. We used the position of Ray 1 as an assay for *mig-32* function. Of transgenic *mig-32(n4275)* mutants carrying the P$_{mig-32}$*mig-32:gfp* reporter (n=50), 28±6% had anterior Ray 1s, compared with 64±5% of *mig-32* mutants (n=100).

To construct the *spat-3a(RNAi)* plasmid, 889 nucleotides of the *spat-3a* genomic region flanking the sequences that encode the RING domain were amplified by PCR and cloned into the L4440 plasmid as a *Hin*dIII-*Bgl*II restriction fragment.

Core histone extraction and western blotting

Packed L1-stage worms (0.5 ml) were harvested from freshly-starved plates. Worms were sonicated in 5 ml NIB buffer [15 mM PIPES (pH 6.8), 5 mM $MgCl_2$, 60 mM KCl, 0.25 M sucrose, 15 mM NaCl, 1 mM $CaCl_2$, 0.8% Triton and protease inhibitors] (Jackson et al., 2004) until the cuticle was completely broken. Lysate was centrifuged at 10,000 ***g*** for 10 minutes. The pellet was resuspended in 2 ml of 0.4 N H_2SO_4 and incubated at 4°C for 1 hour to overnight. The soluble material was dialyzed with PBS or precipitated with 20% TCA. TCA-precipitated histone extract was washed with cold acetone three times and the final pellet dried and dissolved in water. For detection of H2A, rabbit antiserum against histone H2A from Upstate (#07-146) was used at 1/1000 dilution. For detection of ubiquitylated histones, monoclonal anti-ubiquitin (clone P4D1) from Cell Signaling Technology was used at 1/1000 dilution.

RESULTS

MIG-32 is a RING-domain-containing protein homologous to Polycomb group family members, including the core component BMI-1

We identified MIG-32 and SPAT-3A as proteins most similar to core components of the PRC1 complex. As the existence of a PRC1-like complex has been uncertain in *C. elegans*, the genetic pathways in which *mig-32* and *spat-3* might participate are unclear. We therefore identified mutations in *mig-32* and *spat-3* to study their function.

We first confirmed the gene structure predictions for *mig-32* by determining the DNA sequences of five full-length *mig-32* cDNAs, and found that all were identical in the predicted coding sequences and were SL2-spliced, consistent with genome database predictions that *mig-32* is the second gene in a three-gene operon (WormBase, http://www.wormbase.org, release WS193, July, 2008) (Spieth et al., 1993). *mig-32* is predicted to encode a 542 amino acid protein with no close homologs in the completely sequenced *C. elegans* genome, and with a predicted RING domain as the only domain recognized by Pfam (Bateman et al., 2002). Using BLAST searches we identified MIG-32 homologs in vertebrate genomes, including six homologous proteins from humans (Fig. 1). Included in this group are the BMI-1 protein and the related proteins MEL-18/RFP110, NSPc1/PcGRF1 and Pcgf5, which participate in PRC1-related complexes (Alkema et al., 1997; Sanchez et al., 2007; Trimarchi et al., 2001). The *Drosophila melanogaster* genome contains two homologs: *Posterior sex combs*, a component of the *Drosophila* PRC1 complex (Saurin et al., 2001), and *Lethal (3) 73 Ah*, an essential gene (Belote et al., 1990; Irminger-Finger and Nothiger, 1995). We identified a single MIG-32 homolog in the genomic sequences of each of the nematodes *C. briggsae* and *C. remanei* (Fig. 1). These data suggest that MIG-32 is a RING domain protein most similar to core components of human and *Drosophila* PRC1 and related complexes.

We identified three deletion alleles of *mig-32* (see Materials and methods). Each of the alleles deletes *mig-32* genomic coding sequences and not coding sequences of the upstream or downstream genes in the operon. *mig-32(n4275)* mutants, and mutants carrying the *tm1684* and *tm1807* alleles, are homozygous viable and have defects in the male tail and other structures as outlined briefly here and in greater detail below.

The male tail has nine bilateral sensory ray structures (Emmons, 2005). We used the defect in the position of one of these rays to examine the consequences for *mig-32* function of the three deletion alleles. All three alleles result in qualitatively and quantitatively similar defects in the position of Ray 1, with 60-80% of the mutants having an anterior Ray 1; all three also result in similar defects in migration of the HSN neurons (see below). The alleles are recessive, and 75% of mutants of genotype *n4275* over *sDf62*, a chromosomal deficiency that deletes the *mig-32* region, have defects in Ray 1 position similar to those of *mig-32* homozygotes (data not shown).

Three observations suggest that the deletions specifically affect *mig-32* function and not the function of *F11A10.8* or *F11A10.6*, the upstream and downstream genes in the operon, respectively. First, *F11A10.8* encodes a very-well-conserved homolog of human CPSF4, a splicing factor (WormBase). Inactivation of *F11A10.8* by RNAi is lethal, as is a deletion mutation, *ok844*, which deletes parts of the F11A10.8 and *mig-32* coding regions (WormBase), suggesting that the *mig-32(n4275)*, *tm1684* and *tm1807* deletions do not severely impair *F11A10.8* function. Second, RNAi of *mig-32*, which primarily targets processed mRNA (Fire et al., 1998), results

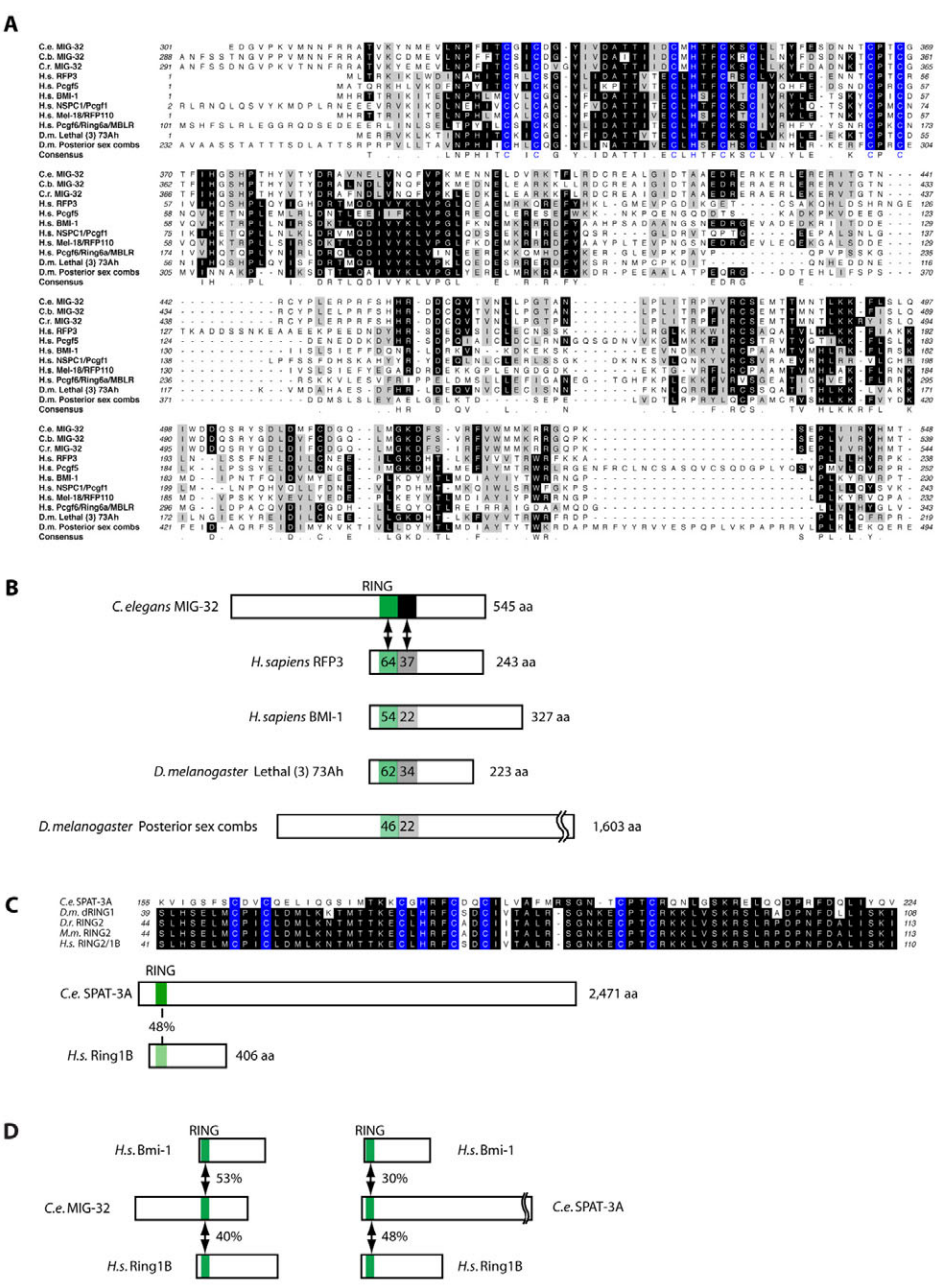

Fig. 1. MIG-32 and SPAT-3A are RING-domain proteins closely related to Polycomb-group family members. Alignment and comparison of MIG-32 and SPAT-3A with related proteins from other species. (**A**) Amino acids highlighted in blue indicate the RING domain. (**B**) MIG-32 compared with related human and *Drosophila* proteins. The green box indicates the RING domain; the black box indicates a C-terminal region that participates in complex formation with RING1B (Li et al., 2006). Percentage amino acid sequence identities (shown as a number within the compared regions) are indicated in pair-wise comparisons between MIG-32 and the other proteins. (**C**) Amino acid sequence alignments of the RING domain of SPAT-3A and dRING1 with related proteins. There is little or no additional sequence similarity between SPAT-3A and RING1B/RING2 homologs from these other species. (**D**) Pair-wise comparisons of the amino acid identities between the RING domains of MIG-32 and SPAT-3A from *C. elegans* with BMI-1 and RING1B from humans.

in an anterior position of Ray 1, as we observed in *mig-32* mutants. Third, expression using the *plx-1* promoter (Dalpe et al., 2004) of a *mig-32* cDNA in the male tail rescued the anterior Ray 1 defects of *mig-32(n4275)* mutants. Specifically, of 50 *mig-32(n4275)* mutants carrying a $P_{plx\text{-}1}$*mig-32:cfp* transgene, 12±5% (standard error of the proportion) had an anterior Ray 1 compared with 64±5% of 100 uninjected controls, and in contrast to *mig-32* mutant males the transgenic males mated efficiently (see below and data not shown). These data suggest that the *n4275*, *tm1684* and *tm1807* alleles are strong loss-of-function or null alleles of *mig-32*. Unless otherwise indicated, we used the *mig-32(n4275)* allele for the experiments described here.

Remarkably, the brood sizes of *mig-32* mutants are similar to those of the wild-type strain, N2. Specifically, the brood sizes of *n4275*, *tm1684* and *tm1807* mutants are 81, 71 and 63% of the wild type. Eggs laid by *mig-32* mutants hatch at rates similar to those of wild-type animals (Table 1 and data not shown).

SPAT-3A is a RING domain protein homologous to the PRC1 core component RING1B

spat-3 was originally identified in RNAi screens as a suppressor of the embryonic polarity gene *par-2*, although the mechanism of suppression is unknown (Labbe et al., 2006). *spat-3* is predicted to encode two large protein products, SPAT-3A and SPAT-3B,

Table 1. Brood sizes of *mig-32* and *spat-3* mutants

Genotype	Avg brood size	*n*
Wild type	234	2,804
mig-32(n4275)	190	2,284
mig-32(tm1807)	167	2,002
mig-32(tm1684)	148	1,775
spat-3(gk22)	209	2,513

The average (Avg) number of progeny was determined for twelve hermaphrodites of the indicated genotypes.
n, total number of progeny.

generated by alternative promoters and supported by partial cDNA evidence (WormBase). The SPAT-3A protein is 2471 amino acids and contains a RING domain at the N-terminus that is most similar to that of the Ring1B proteins of mammals, although the similarity is very poor (Fig. 1). SPAT-3B lacks the RING domain, and neither protein has additional recognized domains. Using the BLAST algorithm, SPAT-3A is the RING domain protein in the *C. elegans* genome most similar to Ring1B; the next most similar protein is MIG-32 (Fig. 1). A deletion allele of *spat-3*, *gk22*, deletes the genomic sequences common to the *spat-3a* and *spat-3b* transcripts, and if transcribed and translated is predicted to truncate the SPAT-3A protein after position 1620. As such, it may represent a loss-of-function but not null allele, as the RING domain is very near the N-terminus (Fig. 1). *spat-3(gk22)* mutants are viable and healthy, with a brood size that is 90% of wild-type animals (Table 1).

MIG-32 and SPAT-3A are required for ubiquitylation of histone H2A

The defined biochemical function of PRC1 is ubiquitylation of histone H2A at position 119. In PRC1, the Ring1B protein serves as the E3 that catalyzes H2A ubiquitylation (Wang et al., 2004a). Other core components, especially BMI-1, stimulate the catalytic activity of Ring1B (Cao et al., 2005; Li et al., 2006; Wei et al., 2006), possibly by promoting folding and stability of Ring1B (Ben-Saadon et al., 2006). We therefore asked whether H2A ubiquitylation was abnormal in *mig-32* and *spat-3* mutants. We analyzed histone modification using western blots of acid-extracted histones from wild-type, *mig-32* and *spat-3* mutant *C. elegans*. Using an H2A-specific antibody and extracts from wild-type animals, we detected H2A and a rare, higher molecular weight band that migrated at the size expected for ubiquitin-modified H2A; this band was not detected in extracts from *mig-32* or *spat-3* mutants (Fig. 2). Using an antibody that detects ubiquitin with histone extracts from wild-type animals, we detected two bands that correspond to the predicted molecular weights of H2A and H2B, both of which are modified by ubiquitylation (Osley, 2006). H2A, the smaller of these bands, is not detected in extracts from *mig-32* mutants and is greatly reduced in *spat-3* mutants (Fig. 2). These data suggest that MIG-32 and SPAT-3A are required for ubiquitylation of Histone H2A, the defining biochemical function of PRC1.

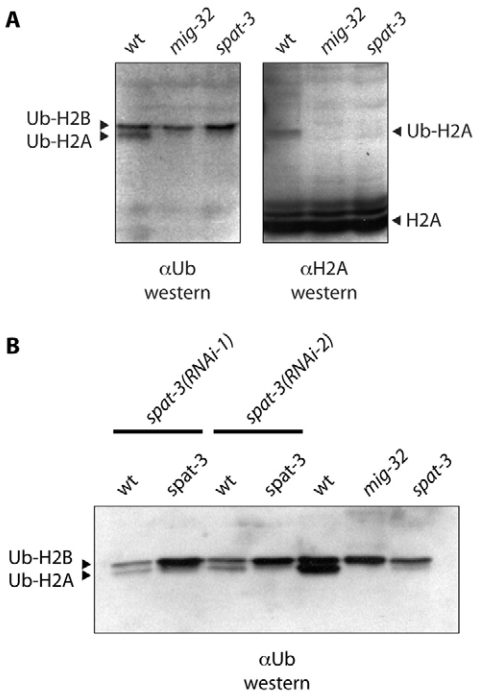

Fig. 2. *mig-32* is required for ubiquitylation of histone H2A. (**A**) Western blot analysis of acid-extracted histones from wild-type, *mig-32(n4275)* and *spat-3(gk22)* mutant *C. elegans*. The filter shown in the left panel was probed with anti-ubiquitin antibody. Arrowheads indicate ubiquitylated H2A and H2B. In the right panel, this blot was stripped and probed with anti-H2A antibody. Arrowheads indicate H2A and ubiquitylated H2A. (**B**) *spat-3* mutants have greatly reduced levels of ubiquitylated H2A. A western blot using anti-ubiquitin antibody detects a trace amount of ubiquitylated H2A in most preparations of acid-extracted histones from *spat-3(gk22)* mutants, consistent with this allele being strong loss-of-function, but not null. A *spat-3(RNAi)* construct was fed to wild-type animals in two experiments [*spat-3(RNAi-1)* and *spat-3(RNAi-2)*]. The RNAi construct reduces, but does not eliminate, ubiquitylated H2A levels. Loading was not equal in all lanes of this blot.

mig-32 is broadly expressed, localized to nuclei and concentrated within nucleoli

In situ hybridization using a *mig-32* cDNA suggested that the gene is expressed prominently in the *C. elegans* germline (Y. Kohara, personal communication). We constructed a rescuing GFP reporter to determine the expression pattern in somatic cells (see Materials and methods). Consistent with MIG-32 acting as a modifier of chromatin, the P_{mig-32}*mig-32:gfp* reporter is expressed broadly in most or all nuclei, beginning early in embryogenesis and continuing in larval development and into adulthood of males and hermaphrodites (Fig. 3 and data not shown). Expression is predominantly nuclear, with relatively bright intranuclear areas of fluorescence that correspond with nucleoli evident as seen with Nomarski optics, particularly in some hypodermal cells where nucleoli are easily identified (Fig. 3). Transfection of mammalian cells with a FLAG-epitope-tagged MIG-32 showed nuclear expression concentrated in a shell around nucleoli, suggesting that the interactions that determine subcellular localization may be evolutionarily conserved (Fig. 3). We considered the possibility that localization of MIG-32 might depend upon *mes* gene activity. To test this, we examined the expression and localization of the P_{mig-32}*mig-32:gfp* reporter in *mes-2* mutants and observed that expression of the reporter is brighter in the *mes-2* mutant background but that the fusion protein remains localized to nuclei and nucleoli (data not shown).

mig-32 and *spat-3* have similar defects in the anatomy of the male tail, and *mig-32* may act with the *mes* genes to position Ray 1

We observed that *mig-32* and *spat-3* mutant males mate very poorly. Observation of the male tail showed that Ray 1 is located abnormally anterior in *mig-32* and *spat-3* mutants, and also in *mig-32(RNAi)* and *spat-3a(RNAi)* animals (Fig. 4). Several genetic pathways position Ray 1 appropriately in males. These include the *mes-2*, *mes-3* and *mes-6* genes, which encode *C. elegans* homologs of the PRC2 histone methyltransferase complex (Bender et al., 2004; Ross and Zarkower, 2003). We constructed double mutants between *mig-32* and putative null alleles of each of the *mes* genes. Strikingly, the Ray 1 position defects of these double mutants were not enhanced (Fig. 4), suggesting that *mig-32* acts in the same genetic pathway as the *mes* genes to position Ray 1.

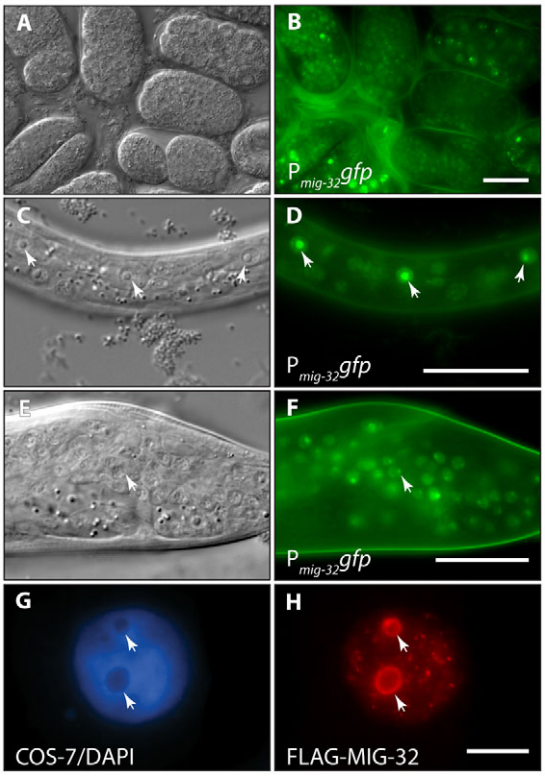

Fig. 3. *mig-32* is broadly expressed, localized to nuclei, and concentrated in nucleoli. Differential interference contrast (A,C,E) and epifluorescence (B,D,F) images of transgenic *C. elegans*. (**A**,**B**) Mixed-stage embryos. (**C**,**D**) L1-stage larva showing the lateral hypodermal cells. Arrowheads highlight nucleoli within hypodermal nuclei. (**E**,**F**) L4-stage male tail. Arrowhead highlights a nucleolus within a neuronal nucleus. (**G**,**H**) COS-7 cell transfected with FLAG-epitope-tagged *C. elegans* MIG-32, stained with (G) DAPI to visualize DNA and (H) anti-FLAG antibody. Arrowheads highlight nucleoli in the COS cell nucleus. In C-F, anterior is to the left and ventral down. Scale bars: 10 μm.

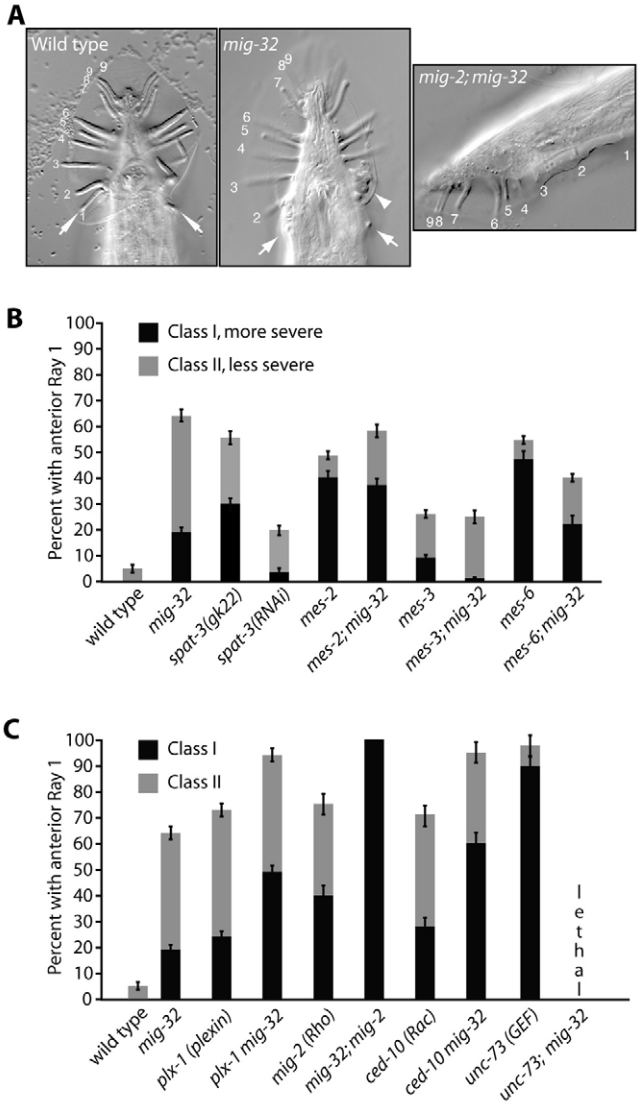

Fig. 4. *mig-32* acts parallel to most known pathways that position Ray 1, with the exception of the PRC2 pathway. (**A**) Ventral views of the tails of male wild-type and *mig-32* mutants and a lateral view of a *mig-2; mig-32* mutant male. The nine bilateral rays are numbered. Arrows indicate Ray 1 pairs in the wild-type and *mig-32* mutants; an arrowhead indicates crumpled Rays 2 and 3 in the *mig-32* mutant. (**B**) The percentage of animals with anterior Ray 1 in wild-type and mutant animals. The severity of the Ray 1 migration defect is categorized as Class I, in which the ray is located anterior to and outside of the normal position of the cuticular fan, or as Class II, in which the ray is anterior but present within the fan (Fujii et al., 2002; Ginzburg et al., 2002). (**C**) The percentage of animals with anterior Ray 1 in wild-type and mutant animals of the indicated genotypes, scored as in B.

Several additional pathways position Ray 1, including signaling by semaphorins and a Plexin receptor (Fujii et al., 2002; Ginzburg et al., 2002), acting through the *unc-73* guanine nucleotide exchange factor and the *ced-10/Rac mig-2/Rho* GTPases (Dalpe et al., 2004). We constructed double mutants between *mig-32* and each of these genes and examined the position of Ray 1 in the male tails of the animals. In each case we identified significantly enhanced defects in the position of Ray 1 (Fig. 4), suggesting that *mig-32* acts parallel to these pathways to position Ray 1.

mig-32 and *spat-3a* are required for HSN neuronal migration and axon extension

We observed that *mig-32* mutants were variably egg-laying defective, with some animals in a population carrying more eggs than wild-type animals. In staged adults the wild-type strain N2 carried an average of 17.5±5 eggs, compared with 28.8±11 eggs in *mig-32* mutants (n=55 animals for each genotype, P<0.0001, unpaired two-tailed t-test). Egg-laying requires a vulva through which the eggs are laid, muscles to expel the eggs, and neurons to control the vulval muscles (Trent et al., 1983). We found that the two HSN neurons, which are essential for egg-laying (Trent et al., 1983), are often abnormal in *mig-32* mutants (Figs 5 and 6). During embryogenesis the HSN neurons migrate from the tail to the midbody (Sulston et al., 1983). Using the $P_{nlp-1}gfp$ reporter to identify the HSN neurons (Li et al., 1999), we observed that the HSNs of *mig-32(n4275)* mutants failed to reach the midbody in 41% of mutants; by comparison, all HSNs migrated to their normal position in otherwise wild-type animals carrying the $P_{nlp-1}gfp$ reporter (Fig. 6). The axons extended by the HSN neurons were also abnormal. In wild-type animals, each HSN

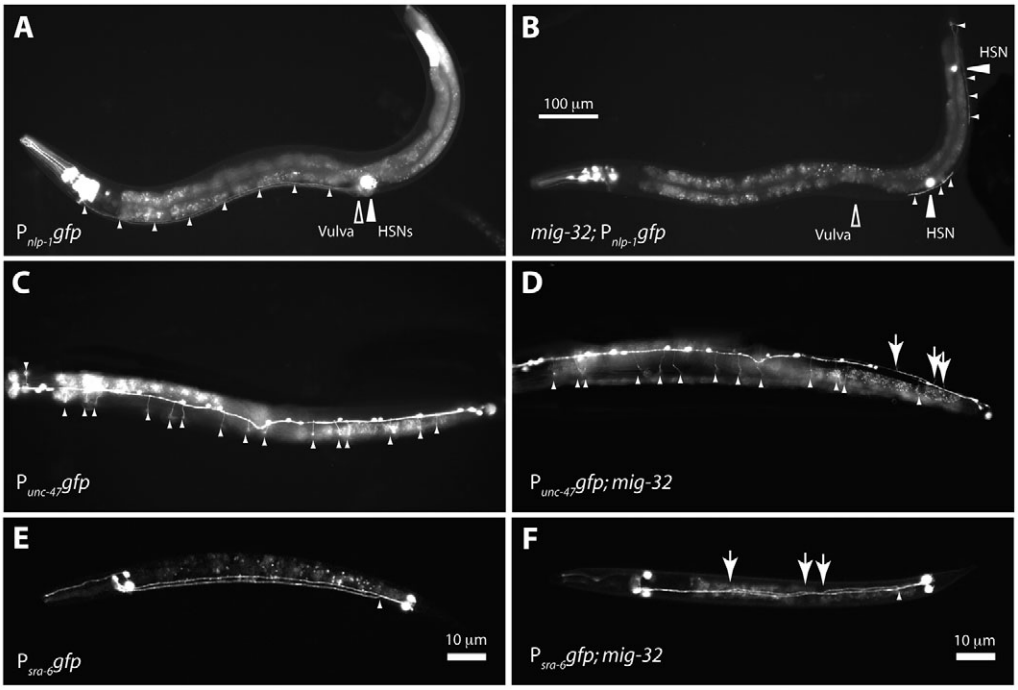

Fig. 5. *mig-32* mutants have defects in neuronal migration and process extension. Images of wild-type and *mig-32* mutant animals carrying *gfp* reporters. (**A**) An otherwise wild-type animal expressing $P_{nlp\text{-}1}gfp$ in the HSN neurons. HSN cell bodies are indicated with a large white arrowhead. The position of the vulva is indicated. Small white arrowheads highlight the axons of the two HSN neurons, which proceed along the ventral body wall to the head. (**B**) A *mig-32* mutant expressing $P_{nlp\text{-}1}gfp$. Large white arrowheads indicate the HSN cell bodies and small arrowheads highlight the HSN axons. (**C**) Ventral view of a wild-type animal expressing $P_{unc\text{-}47}gfp$ in the VD neurons. Small white arrowheads indicate lateral commissures. (**D**) Ventral view of a *mig-32* mutant expressing $P_{unc\text{-}47}gfp$ in the VD neurons. Small white arrowheads indicate lateral commissures. Large arrows indicate three commissures on the wrong side. (**E**) A wild-type animal expressing $P_{sra\text{-}6}gfp$ in the PVQL and PVQR neurons. A small white arrowhead indicates the normal separation of the PVQ axons into the right and left sides of the ventral nerve cord. (**F**) A *mig-32* mutant expressing $P_{sra\text{-}6}gfp$ in the PVQ neurons. Arrows indicate inappropriate crossing by the PVQ neuronal axons. The scale bar in B applies to A-D, which show adult animals. E and F show L1-stage larvae. Anterior is to the left in all images; ventral is down in A and B, up in C and D, and slightly rotated in E and F.

extends an axon from the vulval region ventrally to the ventral nerve cord; the axons then turn anterior and extend to the head. Of the HSN axons of *mig-32* mutants, 56% failed to reach the head; by comparison, all HSN axons extended to the head of otherwise wild-type animals carrying the $P_{nlp\text{-}1}gfp$ reporter (Figs 5 and 6). All HSNs of *mig-32* mutants expressed the $P_{nlp\text{-}1}gfp$ reporter, suggesting that the HSN neurons correctly establish their identity and that the defects in HSN migration result from a requirement for *mig-32* in other processes important for migration and axon extension. The defects in HSN migration and axon extension are likely to account for the variable defects in egg-laying we observed in *mig-32* mutants; such variability has been associated with other mutants with defects in HSN migration (Desai et al., 1988).

mig-32 could have two distinct roles: modification of H2A to regulate gene expression and a developmental role in neuronal migration that is independent of H2A ubiquitylation. If the defects we observed in the nervous system of *mig-32* mutants reflect the role of MIG-32 as part of a PRC1-like complex that includes SPAT-3A, *spat-3* mutants should have defects very similar to those of *mig-32* mutants. Indeed, the HSN neurons of *spat-3* mutants failed to migrate appropriately, and were defective to an extent similar to that observed in *mig-32* mutants (Fig. 6). Like *mig-32* mutants, all HSNs of *spat-3* mutants expressed the $P_{nlp\text{-}1}gfp$ reporter, suggesting that the HSNs of *spat-3* mutants also correctly establish their identity.

mig-32 mutants have additional defects in laterality of commissures, process extension and midline crossing by axons

Using *gfp* reporters, we surveyed *mig-32* mutants for defects in neuronal migration and processes extended by other neurons. The $P_{unc\text{-}47}gfp$ reporter is expressed in the VD and DD motoneurons of the ventral nerve cord (McIntire et al., 1997). In otherwise wild-type animals carrying the $P_{unc\text{-}47}gfp$ reporter, the VD and DD neurons extend commissures from the ventral nerve cord laterally along the body wall to the dorsal nerve cord. In wild-type animals, all but one pair of commissures track along the right side of the animal; only 4% of otherwise wild-type animals carrying the $P_{unc\text{-}47}gfp$ reporter had more than one pair of commissures on the wrong side (Fig. 5; Table 2). By contrast, 63% of *mig-32* mutants had more than two left-sided commissures, with some animals having as many as five commissures on the wrong side (Fig. 5; Table 2). The number and positions of VD and DD neurons, the total number of commissures and the expression of $P_{unc\text{-}47}gfp$ were normal in *mig-32* mutants (data not shown).

We also identified defects in midline crossing by the PVQR and PVQL neurons. The PVQ neurons are located in the lumbar ganglion and each extends an axon anteriorly to the head. Initially, both axons extend along the right side of the hypodermal ridge that divides the ventral nerve cord. The PVQL axon then crosses the midline to the left side and proceeds to the head (White et al., 1986). Using the $P_{sra\text{-}6}gfp$ reporter, which is expressed in the PVQ neurons

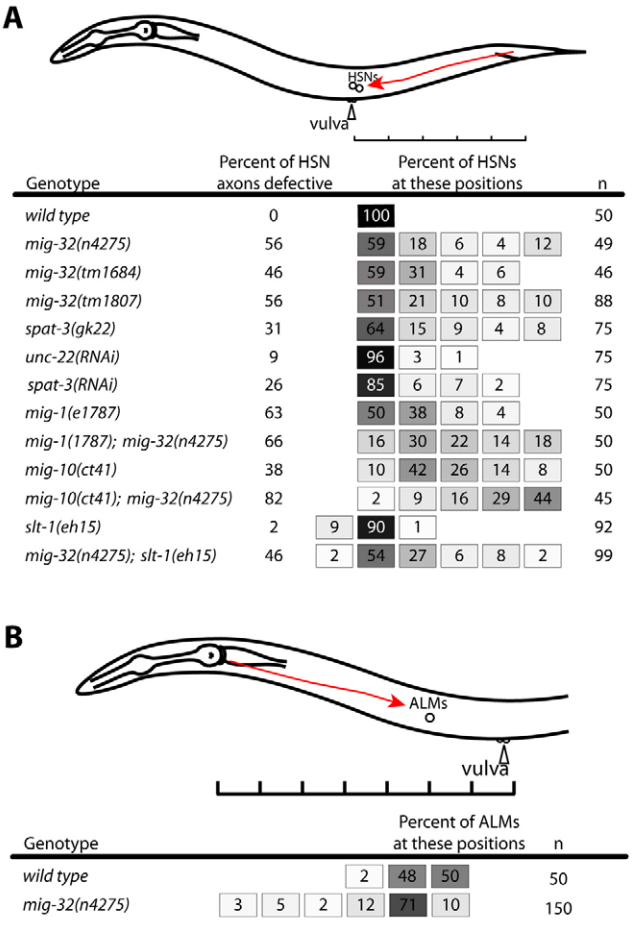

Fig. 6. *mig-32* and *spat-3* act similarly in HSN migration. (**A**) The embryonic migration path (red arrow) and final positions of the HSN neurons in wild-type and mutant transgenic animals. The $P_{nlp\text{-}1}gfp$ reporter, which is expressed in the HSNs (Li et al., 1999), was used to identify the final positions of the HSNs (see Materials and methods). The shaded boxes indicate the percentage of animals with HSNs in specific regions. The percentage of HSN axons that failed to reach the head is shown. n, number of HSNs assayed. (**B**) The migration path (red arrow) and final positions of the ALM neurons. The $P_{mec\text{-}7}gfp$ reporter, which is expressed in the ALMs (Hamelin et al., 1992), identified their final positions.

Table 2. Quantification of process defects in *mig-32* mutants

Genotype	Cell process	Animals with a defect (%)	*n*
$P_{nlp\text{-}1}gfp$	HSN axon	0	50
mig-32(n4275), $P_{nlp\text{-}1}gfp$	HSN axon	56	49
mig-32(tm1684), $P_{nlp\text{-}1}gfp$	HSN axon	46	46
mig-32(tm1807), $P_{nlp\text{-}1}gfp$	HSN axon	56	88
$P_{sra\text{-}6}gfp$	PVQ axons	8	50
mig-32; $P_{sra\text{-}6}gfp$	PVQ axons	26	87
$P_{unc\text{-}47}gfp$	VD commissures	4	25
mig-32; $P_{unc\text{-}47}gfp$	VD commissures	63	100

The percentage of animals with a defect in specific neuronal processes is shown. For the HSN axons, animals were scored as defective if the axon failed to reach the head; in general, axons that reached the head followed a normal path from the HSN ventrally into the ventral nerve cord then turned anterior to the head. HSN neurons that failed to migrate to the midbody often had more severe defects in axon pathfinding, with axons that tracked posterior rather than anterior. For the PVQ axons, defective axons included those that crossed the midline inappropriately, as compared with wild-type animals. For the VD commissures, defective commissures included those that tracked on the wrong side of the body wall. *mig-32* mutants had 0-5 commissures on the wrong side, with posterior VD neurons being more likely to have defective commissures.

(Troemel et al., 1995), we observed that the PVQ axons of *mig-32* mutants did not respect the midline boundary and crossed inappropriately (Fig. 5; Table 2). Of the PVQ axons of *mig-32* mutants, 26% crossed the midline inappropriately, compared with 8% of otherwise wild-type animals carrying the $P_{sra\text{-}6}gfp$ reporter. All PVQ neurons of *mig-32* mutants expressed $P_{sra\text{-}6}gfp$ at levels similar to wild-type animals.

Some neurons and axons of *mig-32* mutants migrated and extended processes normally, whereas others were slightly abnormal. The CAN neurons originate in the head and migrate posteriorly to a position adjacent to the vulva. Using a $P_{ceh\text{-}23}gfp$ reporter, we observed that all 50 CAN neurons of *mig-32* mutants migrated appropriately and extended axons as in the wild type (data not shown). Several of the mechanosensory neurons migrate along the anteroposterior body axis during development (Hamelin et al., 1992). The Q cells migrate anteriorly and divide, with the QR cell (right-sided Q cell) generating the AVM mechanosensory neuron and QL (left-sided Q cell) the PVM neuron. The ALM neurons migrate posteriorly from the head. Using the $P_{mec\text{-}7}gfp$ reporter to label the mechanosensory neurons and their axons, we found that the ALM neurons of *mig-32* mutants were slightly defective in posterior migration. Of 150 ALM neurons observed in *mig-32* mutants, 15 ALMs did not complete their migrations (Fig. 6). The processes of the ALM neurons were similar in *mig-32* and wild-type animals (data not shown). The PLM neurons did not migrate, but their posterior processes were often foreshortened in *mig-32* mutants. Of 100 PLM neurons of *mig-32* mutants, the posterior process terminated prematurely in 55% of animals, extending less than half the normal distance. By contrast, the posterior processes of the PLM neurons terminated prematurely in only 6% of 100 wild-type animals. The locations of the AVM and PVM neurons and the morphology of their processes were similar, comparing 75 *mig-32* mutants with 50 wild-type animals (data not shown).

Migration of the distal tip cells, which are somatic cells that lead the anterior and posterior arms of the proliferating germline along the body wall, appeared normal, comparing 23 *mig-32* mutants with 18 wild-type animals (data not shown).

In summary, *mig-32* is required for normal migration of the HSN neurons and for extension of some neuronal processes. It participates in ensuring that VD neuronal commissures extend along the correct side of the animal, and that the PVQ axons do not cross the midline inappropriately. The defects we observed in *mig-32* mutants are unlikely to be a result of markedly altered neuronal differentiation, because expression of all the *gfp* reporters used for these experiments were expressed in the expected patterns in *mig-32* mutants (a list of reporters used is found in Materials and methods).

mig-32 acts parallel to most known pathways that act in HSN migration

Several genetic pathways have been identified that ensure correct migration of the HSN neurons from the tail to the vulva. To determine whether *mig-32* acts within one of these pathways, we constructed double mutants between *mig-32* and other genes that regulate HSN migration, including *mig-1*, a Wnt receptor and *Frizzled* homolog (Pan et al., 2006), *mig-10*, a cytoplasmic protein that mediates attractive and repulsive guidance signals by *unc-6*/Netrin and *slt-1* (Chang et al., 2006; Quinn et al., 2006), respectively, and *slt-1* (Hao et al., 2001). In each case, the double

mutants with *mig-32* had significantly enhanced defects in HSN migration assayed with the $P_{nlp\text{-}1}gfp$ reporter (Fig. 6). These data suggest that *mig-32* acts genetically parallel to these pathways to promote HSN migration.

mig-32 and *spat-3* repress ectopic vulval development

The *lin-15* locus is an operon that includes two genes, *lin-15A* and *lin-15B*, both of which are redundant repressors of a vulval fate for hypodermal descendants of the P cells in the vulval equivalence group (Clark et al., 1994). Mutants carrying the temperature-sensitive allele *n765* are morphologically normal when raised at 15°C but show a multiple vulva (Muv) phenotype when raised at 20°C; the *lin-15(n765ts)* allele has a single mutation that impairs function of both *lin-15A* and *lin-15B* (Cui et al., 2008). During strain constructions, we observed that *mig-32; lin-15(n765ts)* double mutants are 100% Muv at 15°C (data not shown). We used this observation to test whether *spat-3* and *mig-32* might act similarly to repress vulval fates. We subjected *lin-15(n765ts)* mutants to *mig-32(RNAi)* or *spat-3a(RNAi)* and raised the animals at 15°C; the *spat-3a(RNAi)* construct specifically targeted the *spat-3a* transcript that encodes the RING domain. Reducing either *mig-32* or *spat-3a* activity resulted in a highly penetrant Muv phenotype. Seventy-three percent of *lin-15(n765ts); mig-32(RNAi)* mutants (n=320) and 42% of *lin-15(n765ts); spat-3(RNAi)* mutants (n=200) were Muv, compared with 3% of *lin-15(n765ts); unc-22(RNAi)* mutants (n=100). These data suggest that *mig-32* and *spat-3a* act similarly to repress vulval fates in hypodermal cells that do not normally contribute to vulval development.

DISCUSSION

In this manuscript we report the consequences for *C. elegans* of the loss of two proteins homologous to core subunits of the PRC1 complex, MIG-32 and SPAT-3A. MIG-32 and SPAT-3A are most similar to families of proteins that include Bmi-1 and Ring1B, respectively. In mammals, Ring1B is the E3 ligase in PRC1 that modifies H2A, and BMI-1 is a physical partner of Ring1B that promotes the stability and catalytic activity of Ring1B (Cao et al., 2005; Li et al., 2006; Wang et al., 2004a; Wang et al., 2004b). Consistent with MIG-32 and SPAT-3A acting together in a PRC1-like complex, *mig-32* and *spat-3* mutants are markedly defective in H2A ubiquitylation and have very similar defects in the anatomy of their nervous systems and as repressors of ectopic vulval fates in hypodermal cells. We therefore propose that MIG-32 and SPAT-3A are core subunits of a PRC1-like complex in *C. elegans*, although we have not yet demonstrated complex formation by these proteins.

The relationship of MIG-32 and SPAT-3A with PcG complexes of *C. elegans*

There are at least two complexes in *C. elegans* that are functionally related to the *Drosophila* and mammalian Polycomb repression complexes. Strong genetic and biochemical evidence indicates that the MES-2–MES-3–MES-6 complex is functionally analogous to the PRC2 complex (Xu et al., 2001a), which places the histone H3K27me3 mark characteristic of Polycomb repression (Bender et al., 2004; Fong et al., 2002; Holdeman et al., 1998; Xu et al., 2001a). *mes* mutants are sterile, probably as a consequence of inappropriate expression of genes normally silenced in the developing germ cells. If PRC1 were required for regulation of gene expression by PRC2, *mig-32* and *spat-3* mutants might be expected to share the Mes phenotype of sterility. However, both mutants are healthy and fertile. *mig-32* and *spat-3* could be redundant with other proteins or complexes responsible for H2A ubiquitylation in the germline, or H2A ubiquitylation could be dispensable for the silencing function that is thought to be the essential role of the *mes* genes in ensuring germline integrity. We favor the latter possibility, as western blots of L1-stage wild-type animals with rudimentary germlines have relatively high steady state levels of ubiquitylated H2A and H2B, but we detected little ubiquitylated histone in L4 or young adult animals with proliferative germlines (our unpublished observations).

More recently the *sop-2*, *sor-1* and *sor-3* genes have been proposed as components of a distinct Polycomb complex-like repressive mechanism in *C. elegans*. Mutations affecting these genes result in expanded domains of Hox gene expression (Wang et al., 2004a; Yang et al., 2007; Zhang et al., 2003; Zhang et al., 2004). All are essential genes, and mutants carrying partial loss-of-function alleles have severe defects not observed in *mes* null mutants, suggesting that the *sop* and *sor* genes have many important functions in somatic cells and do not simply maintain the pattern of gene expression established by the *mes* genes, which have subtle functions in somatic cells (Ross and Zarkower, 2003). The pattern of nuclear fluorescence we observed for a rescuing MIG-32:GFP fusion protein suggests that MIG-32 does not co-localize with the SOP-2 and SOR-1 proteins (Saurin et al., 1998; Yang et al., 2007; Zhang et al., 2006). Given the numerous and severe defects of the *sop* and *sor* mutants and the comparatively limited defects of *mig-32* and *spat-3* mutants, MIG-32 and SPAT-3A are unlikely to be essential components of a putative SOP/SOR Polycomb-like complex.

The roles of Polycomb complexes in nervous system development

The *mig-32* homolog *Bmi-1* has been intensively studied following its isolation as a target gene upregulated by proviral integration in Eμ-myc-driven lymphomas in mice (Haupt et al., 1991; van Lohuizen et al., 1991). In the mammalian nervous system *Bmi-1* is required for the self-renewal of neural stem cells (Molofsky et al., 2005; Molofsky et al., 2003), and epigenetic regulation of the cell cycle is a crucial function of *Bmi-1* in the hematopoietic and nervous systems (Jacobs et al., 1999; Molofsky et al., 2005; Molofsky et al., 2003). We have not observed abnormalities in cell numbers in *mig-32* mutants that would suggest an essential role in the regulation of the cell cycle, but we have not directly examined this possibility.

Expression of additional MIG-32 homologs in the mammalian nervous system has been reported (Gunster et al., 1997; Jacobs et al., 1999; Kim et al., 2005; Leung et al., 2004; Molofsky et al., 2003; Nunes et al., 2001; Schoorlemmer et al., 1997; Shakhova et al., 2005; van der Lugt et al., 1994), but with the exception of *Bmi-1* little is known about what these genes contribute to nervous system function. Our data suggest that epigenetic regulation of gene expression by PRC1 and related complexes will participate in neuronal migration and process extension, but the precise basis for the defects we observe in *mig-32* and *spat-3* mutants is not yet clear. Specifically, does PRC1 regulate transcription of individual gene targets that are crucial regulators of individual cell migrations or process extensions, or does loss of PRC1 result in a ‘noisy’ pattern of gene expression to which some cells are more sensitive? Recent genomic screens in *Drosophila* and vertebrates have identified targets of Polycomb repression complexes (Boyer et al., 2006; Bracken et al., 2006; Lee et al., 2006; Negre et al., 2006; Schwartz et al., 2006; Tolhuis et al., 2006). Many of these biochemically defined targets are involved in nervous system patterning, and our data raise the possibility that Polycomb-group complexes regulate these targets

in a functionally important way in the developing nervous system. Our observation that most cells appear to adopt fates similar to those of wild-type animals, as suggested by normal expression of the cell-type-specific *gfp* reporters used in this study, suggests that *mig-32* is not crucial for establishing cell fates, but instead acts in a subtle manner to refine cellular phenotypes.

Defects in Hox gene expression are unlikely to be central for the *mig-32* or *spat-3a* mutant phenotypes

Mutations affecting Hox genes result in abnormal neuronal migrations in *C. elegans* (Baum et al., 1999; Chalfie and Sulston, 1981; Chisholm, 1991; Clark et al., 1993; Harris et al., 1996; Kenyon, 1986; Salser and Kenyon, 1992; Wang et al., 1993), and given the classical role of Polycomb family members as repressors of Hox gene activity we asked whether abnormal Hox gene activity might underlie the defects in the nervous system we observed. However, our data suggest that regulation of Hox gene expression by *mig-32* and *spat-3* may be subtle. In general, the migration and neuronal process extension defects of *mig-32* and *spat-3* mutants have little in common with those observed in gain- or loss-of-function Hox mutants. In addition, the expression domains of the $P_{egl\text{-}5}$*gfp* Hox and $P_{pkd\text{-}2}$*gfp* reporters do not appear to be expanded in *mig-32* mutants, and *mig-32* mutations do not suppress *pal-1* mutations, which reduce Hox activity (our unpublished observations). These data suggest that non-Hox targets of *mig-32* and *spat-3* are more likely to be responsible for the defects we describe, and are consistent with the Polycomb-group targets of *Drosophila* and mammalian cells, the vast majority of which are not Hox genes. However, our data do not rule out a role for MIG-32 or SPAT-3A as regulators of Hox gene activity, and further work to define the genetic and biochemical properties of *mig-32* and *spat-3* in germline and somatic cells will allow comparison to the Polycomb group complexes of other species.

We thank Jean Maines and Leon Avery for comments on the manuscript. We also thank Yuji Kohara for *mig-32* cDNAs, the Mitani laboratory for the *mig-32(tm1807) and tm1684* deletion alleles, the Horvitz lab for the *mig-32(n4275)* deletion allele, and the CGC for many nematode strains used in this work (the CGC is funded by the NIH National Center for Research Resources). This work was supported by NIH grant GM069667 to S.C. Deposited in PMC for release after 12 months.

References

Alkema, M. J., Bronk, M., Verhoeven, E., Otte, A., van't Veer, L. J., Berns, A. and van Lohuizen, M. (1997). Identification of Bmi1-interacting proteins as constituents of a multimeric mammalian polycomb complex. *Genes Dev.* **11**, 226-240.

Bateman, A., Birney, E., Cerruti, L., Durbin, R., Etwiller, L., Eddy, S. R., Griffiths-Jones, S., Howe, K. L., Marshall, M. and Sonnhammer, E. L. (2002). The Pfam protein families database. *Nucleic Acids Res.* **30**, 276-280.

Baum, P. D., Guenther, C., Frank, C. A., Pham, B. V. and Garriga, G. (1999). The *Caenorhabditis elegans* gene *ham-2* links Hox patterning to migration of the HSN motor neuron. *Genes Dev.* **13**, 472-483.

Belote, J. M., Hoffmann, F. M., McKeown, M., Chorsky, R. L. and Baker, B. S. (1990). Cytogenetic analysis of chromosome region 73AD of *Drosophila melanogaster*. *Genetics* **125**, 783-793.

Ben-Saadon, R., Zaaroor, D., Ziv, T. and Ciechanover, A. (2006). The polycomb protein Ring1B generates self atypical mixed ubiquitin chains required for its in vitro histone H2A ligase activity. *Mol. Cell* **24**, 701-711.

Bender, L. B., Cao, R., Zhang, Y. and Strome, S. (2004). The MES-2/MES-3/MES-6 complex and regulation of histone H3 methylation in *C. elegans*. *Curr. Biol.* **14**, 1639-1643.

Boyer, L. A., Plath, K., Zeitlinger, J., Brambrink, T., Medeiros, L. A., Lee, T. I., Levine, S. S., Wernig, M., Tajonar, A., Ray, M. K. et al. (2006). Polycomb complexes repress developmental regulators in murine embryonic stem cells. *Nature* **441**, 349-353.

Bracken, A. P., Dietrich, N., Pasini, D., Hansen, K. H. and Helin, K. (2006). Genome-wide mapping of Polycomb target genes unravels their roles in cell fate transitions. *Genes Dev.* **20**, 1123-1136.

Brenner, S. (1974). The genetics of *Caenorhabditis elegans*. *Genetics* **77**, 71-94.

Cameron, S., Clark, S. G., McDermott, J. B., Aamodt, E. and Horvitz, H. R. (2002). PAG-3, a Zn-finger transcription factor, determines neuroblast fate in *C. elegans*. *Development* **129**, 1763-1774.

Cao, R., Wang, L., Wang, H., Xia, L., Erdjument-Bromage, H., Tempst, P., Jones, R. S. and Zhang, Y. (2002). Role of histone H3 lysine 27 methylation in Polycomb-group silencing. *Science* **298**, 1039-1043.

Cao, R., Tsukada, Y. and Zhang, Y. (2005). Role of Bmi-1 and Ring1A in H2A ubiquitylation and Hox gene silencing. *Mol. Cell* **20**, 845-854.

Capowski, E. E., Martin, P., Garvin, C. and Strome, S. (1991). Identification of grandchildless loci whose products are required for normal germ-line development in the nematode *Caenorhabditis elegans*. *Genetics* **129**, 1061-1072.

Chalfie, M. and Sulston, J. (1981). Developmental genetics of the mechanosensory neurons of *Caenorhabditis elegans*. *Dev. Biol.* **82**, 358-370.

Chang, C., Adler, C. E., Krause, M., Clark, S. G., Gertler, F. B., Tessier-Lavigne, M. and Bargmann, C. I. (2006). MIG-10/lamellipodin and AGE-1/PI3K promote axon guidance and outgrowth in response to slit and netrin. *Curr. Biol.* **16**, 854-862.

Chisholm, A. (1991). Control of cell fate in the tail region of *C. elegans* by the gene *egl-5*. *Development* **111**, 921-932.

Clark, S. G., Chisholm, A. D. and Horvitz, H. R. (1993). Control of cell fates in the central body region of *C. elegans* by the homeobox gene *lin-39*. *Cell* **74**, 43-55.

Clark, S. G., Lu, X. and Horvitz, H. R. (1994). The *Caenorhabditis elegans* locus *lin-15*, a negative regulator of a tyrosine kinase signaling pathway, encodes two different proteins. *Genetics* **137**, 987-997.

Cui, M., Allen, M. A., Larsen, A., Macmorris, M., Han, M. and Blumenthal, T. (2008). Genes involved in pre-mRNA 3′-end formation and transcription termination revealed by a *lin-15* operon Muv suppressor screen. *Proc. Natl. Acad. Sci. USA* **105**, 16665-16670.

Czermin, B., Melfi, R., McCabe, D., Seitz, V., Imhof, A. and Pirrotta, V. (2002). Drosophila enhancer of Zeste/ESC complexes have a histone H3 methyltransferase activity that marks chromosomal Polycomb sites. *Cell* **111**, 185-196.

Dalpe, G., Zhang, L. W., Zheng, H. and Culotti, J. G. (2004). Conversion of cell movement responses to Semaphorin-1 and Plexin-1 from attraction to repulsion by lowered levels of specific RAC GTPases in *C. elegans*. *Development* **131**, 2073-2088.

Desai, C., Garriga, G., McIntire, S. L. and Horvitz, H. R. (1988). A genetic pathway for the development of the *Caenorhabditis elegans* HSN motor neurons. *Nature* **336**, 638-646.

Emmons, S. W. (2005). Male development. In *WormBook* (ed. The *C. elegans* Research Community). www.wormbook.org.

Fire, A., Xu, S., Montgomery, M. K., Kostas, S. A., Driver, S. E. and Mello, C. C. (1998). Potent and specific genetic interference by double-stranded RNA in *Caenorhabditis elegans*. *Nature* **391**, 806-811.

Fong, Y., Bender, L., Wang, W. and Strome, S. (2002). Regulation of the different chromatin states of autosomes and X chromosomes in the germ line of *C. elegans*. *Science* **296**, 2235-2238.

Francis, N. J., Kingston, R. E. and Woodcock, C. L. (2004). Chromatin compaction by a polycomb group protein complex. *Science* **306**, 1574-1577.

Fujii, T., Nakao, F., Shibata, Y., Shioi, G., Kodama, E., Fujisawa, H. and Takagi, S. (2002). *Caenorhabditis elegans* PlexinA, PLX-1, interacts with transmembrane semaphorins and regulates epidermal morphogenesis. *Development* **129**, 2053-2063.

Ginzburg, V. E., Roy, P. J. and Culotti, J. G. (2002). Semaphorin 1a and semaphorin 1b are required for correct epidermal cell positioning and adhesion during morphogenesis in *C. elegans*. *Development* **129**, 2065-2078.

Gunster, M. J., Satijn, D. P., Hamer, K. M., den Blaauwen, J. L., de Bruijn, D., Alkema, M. J., van Lohuizen, M., van Driel, R. and Otte, A. P. (1997). Identification and characterization of interactions between the vertebrate polycomb-group protein BMI1 and human homologs of polyhomeotic. *Mol. Cell. Biol.* **17**, 2326-2335.

Hamelin, M., Scott, I. M., Way, J. C. and Culotti, J. G. (1992). The *mec-7* beta-tubulin gene of *Caenorhabditis elegans* is expressed primarily in the touch receptor neurons. *EMBO J.* **11**, 2885-2893.

Hao, J. C., Yu, T. W., Fujisawa, K., Culotti, J. G., Gengyo-Ando, K., Mitani, S., Moulder, G., Barstead, R., Tessier-Lavigne, M. and Bargmann, C. I. (2001). *C. elegans* slit acts in midline, dorsal-ventral, and anterior-posterior guidance via the SAX-3/Robo receptor. *Neuron* **32**, 25-38.

Harris, J., Honigberg, L., Robinson, N. and Kenyon, C. (1996). Neuronal cell migration in *C. elegans*: regulation of Hox gene expression and cell position. *Development* **122**, 3117-3131.

Haupt, Y., Alexander, W. S., Barri, G., Klinken, S. P. and Adams, J. M. (1991). Novel zinc finger gene implicated as myc collaborator by retrovirally accelerated lymphomagenesis in *E mu-myc* transgenic mice. *Cell* **65**, 753-763.

Holdeman, R., Nehrt, S. and Strome, S. (1998). MES-2, a maternal protein essential for viability of the germline in *Caenorhabditis elegans*, is homologous to a Drosophila Polycomb group protein. *Development* **125**, 2457-2467.
Hunter, C. P., Harris, J. M., Maloof, J. N. and Kenyon, C. (1999). Hox gene expression in a single *Caenorhabditis elegans* cell is regulated by a caudal homolog and intercellular signals that inhibit wnt signaling. *Development* **126**, 805-814.
Irminger-Finger, I. and Nothiger, R. (1995). The *Drosophila melanogaster* gene *lethal(3)73Ah* encodes a ring finger protein homologous to the oncoproteins MEL-18 and BMI-1. *Gene* **163**, 203-208.
Jackson, J. P., Johnson, L., Jasencakova, Z., Zhang, X., PerezBurgos, L., Singh, P. B., Cheng, X., Schubert, I., Jenuwein, T. and Jacobsen, S. E. (2004). Dimethylation of histone H3 lysine 9 is a critical mark for DNA methylation and gene silencing in Arabidopsis thaliana. *Chromosoma* **112**, 308-315.
Jacobs, J. J., Kieboom, K., Marino, S., DePinho, R. A. and van Lohuizen, M. (1999). The oncogene and Polycomb-group gene *bmi-1* regulates cell proliferation and senescence through the *ink4a* locus. *Nature* **397**, 164-168.
Kennison, J. A. and Tamkun, J. W. (1988). Dosage-dependent modifiers of polycomb and antennapedia mutations in Drosophila. *Proc. Natl. Acad. Sci. USA* **85**, 8136-8140.
Kenyon, C. (1986). A gene involved in the development of the posterior body region of *C. elegans*. *Cell* **46**, 477-487.
Kim, M. H., Gunnersen, J. M. and Tan, S. S. (2005). *Mph2* expression in germinal zones of the mouse brain. *Dev. Dyn.* **232**, 209-215.
King, I. F., Francis, N. J. and Kingston, R. E. (2002). Native and recombinant polycomb group complexes establish a selective block to template accessibility to repress transcription *in vitro*. *Mol. Cell. Biol.* **22**, 7919-7928.
Kuzmichev, A., Nishioka, K., Erdjument-Bromage, H., Tempst, P. and Reinberg, D. (2002). Histone methyltransferase activity associated with a human multiprotein complex containing the Enhancer of Zeste protein. *Genes Dev.* **16**, 2893-2905.
Labbe, J. C., Pacquelet, A., Marty, T. and Gotta, M. (2006). A genomewide screen for suppressors of *par-2* uncovers potential regulators of PAR protein-dependent cell polarity in *Caenorhabditis elegans*. *Genetics* **174**, 285-295.
Lee, T. I., Jenner, R. G., Boyer, L. A., Guenther, M. G., Levine, S. S., Kumar, R. M., Chevalier, B., Johnstone, S. E., Cole, M. F., Isono, K. et al. (2006). Control of developmental regulators by Polycomb in human embryonic stem cells. *Cell* **125**, 301-313.
Leung, C., Lingbeek, M., Shakhova, O., Liu, J., Tanger, E., Saremaslani, P., Van Lohuizen, M. and Marino, S. (2004). *Bmi1* is essential for cerebellar development and is overexpressed in human medulloblastomas. *Nature* **428**, 337-341.
Levine, S. S., Weiss, A., Erdjument-Bromage, H., Shao, Z., Tempst, P. and Kingston, R. E. (2002). The core of the polycomb repressive complex is compositionally and functionally conserved in flies and humans. *Mol. Cell. Biol.* **22**, 6070-6078.
Lewis, E. B. (1978). A gene complex controlling segmentation in Drosophila. *Nature* **276**, 565-570.
Li, C., Nelson, L. S., Kim, K., Nathoo, A. and Hart, A. C. (1999). Neuropeptide gene families in the nematode *Caenorhabditis elegans*. *Ann. NY Acad. Sci.* **897**, 239-252.
Li, Z., Cao, R., Wang, M., Myers, M. P., Zhang, Y. and Xu, R. M. (2006). Structure of a Bmi-1-Ring1B polycomb group ubiquitin ligase complex. *J. Biol. Chem.* **281**, 20643-20649.
McIntire, S. L., Reimer, R. J., Schuske, K., Edwards, R. H. and Jorgensen, E. M. (1997). Identification and characterization of the vesicular GABA transporter. *Nature* **389**, 870-876.
Molofsky, A. V., He, S., Bydon, M., Morrison, S. J. and Pardal, R. (2005). Bmi-1 promotes neural stem cell self-renewal and neural development but not mouse growth and survival by repressing the p16Ink4a and p19Arf senescence pathways. *Genes Dev.* **19**, 1432-1437.
Molofsky, A. V., Pardal, R., Iwashita, T., Park, I. K., Clarke, M. F. and Morrison, S. J. (2003). Bmi-1 dependence distinguishes neural stem cell self-renewal from progenitor proliferation. *Nature* **425**, 962-967.
Muller, J., Hart, C. M., Francis, N. J., Vargas, M. L., Sengupta, A., Wild, B., Miller, E. L., O'Connor, M. B., Kingston, R. E. and Simon, J. A. (2002). Histone methyltransferase activity of a Drosophila Polycomb group repressor complex. *Cell* **111**, 197-208.
Negre, N., Hennetin, J., Sun, L. V., Lavrov, S., Bellis, M., White, K. P. and Cavalli, G. (2006). Chromosomal distribution of PcG proteins during Drosophila development. *PLoS Biol.* **4**, e170.
Nunes, M., Blanc, I., Maes, J., Fellous, M., Robert, B. and McElreavey, K. (2001). *NSPc1*, a novel mammalian Polycomb gene, is expressed in neural crest-derived structures of the peripheral nervous system. *Mech. Dev.* **102**, 219-222.
Nusslein-Volhard, C., Kluding, H. and Jurgens, G. (1985). Genes affecting the segmental subdivision of the Drosophila embryo. *Cold Spring Harb. Symp. Quant. Biol.* **50**, 145-154.
Osley, M. A. (2006). Regulation of histone H2A and H2B ubiquitylation. *Brief. Funct. Genomic. Proteomic.* **5**, 179-189.
Pan, C. L., Howell, J. E., Clark, S. G., Hilliard, M., Cordes, S., Bargmann, C. I. and Garriga, G. (2006). Multiple Wnts and frizzled receptors regulate anteriorly directed cell and growth cone migrations in *Caenorhabditis elegans*. *Dev. Cell* **10**, 367-377.
Pujol, N., Torregrossa, P., Ewbank, J. J. and Brunet, J. F. (2000). The homeodomain protein CePHOX2/CEH-17 controls antero-posterior axonal growth in *C. elegans*. *Development* **127**, 3361-3371.
Quinn, C. C., Pfeil, D. S., Chen, E., Stovall, E. L., Harden, M. V., Gavin, M. K., Forrester, W. C., Ryder, E. F., Soto, M. C. and Wadsworth, W. G. (2006). UNC-6/netrin and SLT-1/slit guidance cues orient axon outgrowth mediated by MIG-10/RIAM/lamellipodin. *Curr. Biol.* **16**, 845-853.
Ross, J. M. and Zarkower, D. (2003). Polycomb group regulation of Hox gene expression in *C. elegans*. *Dev. Cell* **4**, 891-901.
Salser, S. J. and Kenyon, C. (1992). Activation of a *C. elegans* Antennapedia homologue in migrating cells controls their direction of migration. *Nature* **355**, 255-258.
Sanchez, C., Sanchez, I., Demmers, J. A., Rodriguez, P., Strouboulis, J. and Vidal, M. (2007). Proteomics analysis of Ring1B/Rnf2 interactors identifies a novel complex with the Fbxl10/Jhdm1B histone demethylase and the Bcl6 interacting corepressor. *Mol. Cell Proteomics* **6**, 820-834.
Saurin, A. J., Shiels, C., Williamson, J., Satijn, D. P., Otte, A. P., Sheer, D. and Freemont, P. S. (1998). The human polycomb group complex associates with pericentromeric heterochromatin to form a novel nuclear domain. *J. Cell Biol.* **142**, 887-898.
Saurin, A. J., Shao, Z., Erdjument-Bromage, H., Tempst, P. and Kingston, R. E. (2001). A Drosophila Polycomb group complex includes Zeste and dTAFII proteins. *Nature* **412**, 655-660.
Schoorlemmer, J., Marcos-Gutierrez, C., Were, F., Martinez, R., Garcia, E., Satijn, D. P., Otte, A. P. and Vidal, M. (1997). Ring1A is a transcriptional repressor that interacts with the Polycomb-M33 protein and is expressed at rhombomere boundaries in the mouse hindbrain. *EMBO J.* **16**, 5930-5942.
Schwartz, Y. B., Kahn, T. G., Nix, D. A., Li, X. Y., Bourgon, R., Biggin, M. and Pirrotta, V. (2006). Genome-wide analysis of Polycomb targets in *Drosophila melanogaster*. *Nat. Genet.* **38**, 700-705.
Shakhova, O., Leung, C. and Marino, S. (2005). Bmi1 in development and tumorigenesis of the central nervous system. *J. Mol. Med.* **83**, 596-600.
Shao, Z., Raible, F., Mollaaghababa, R., Guyon, J. R., Wu, C. T., Bender, W. and Kingston, R. E. (1999). Stabilization of chromatin structure by PRC1, a Polycomb complex. *Cell* **98**, 37-46.
Simon, J., Chiang, A. and Bender, W. (1992). Ten different Polycomb group genes are required for spatial control of the abdA and AbdB homeotic products. *Development* **114**, 493-505.
Spieth, J., Brooke, G., Kuersten, S., Lea, K. and Blumenthal, T. (1993). Operons in *C. elegans*: polycistronic mRNA precursors are processed by *trans*-splicing of SL2 to downstream coding regions. *Cell* **73**, 521-532.
Sulston, J. E., Schierenberg, E., White, J. G. and Thomson, J. N. (1983). The embryonic cell lineage of the nematode *Caenorhabditis elegans*. *Dev. Biol.* **100**, 64-119.
Tolhuis, B., de Wit, E., Muijrers, I., Teunissen, H., Talhout, W., van Steensel, B. and van Lohuizen, M. (2006). Genome-wide profiling of PRC1 and PRC2 Polycomb chromatin binding in *Drosophila melanogaster*. *Nat. Genet.* **38**, 694-699.
Trent, C., Tsung, N. and Horvitz, H. R. (1983). Egg-laying defective mutants of the nematode *Caenorhabditis elegans*. *Genetics* **104**, 619-647.
Trimarchi, J. M., Fairchild, B., Wen, J. and Lees, J. A. (2001). The E2F6 transcription factor is a component of the mammalian Bmi1-containing polycomb complex. *Proc. Natl. Acad. Sci. USA* **98**, 1519-1524.
Troemel, E. R., Chou, J. H., Dwyer, N. D., Colbert, H. A. and Bargmann, C. I. (1995). Divergent seven transmembrane receptors are candidate chemosensory receptors in *C. elegans*. *Cell* **83**, 207-218.
van der Lugt, N. M., Domen, J., Linders, K., van Roon, M., Robanus-Maandag, E., te Riele, H., van der Valk, M., Deschamps, J., Sofroniew, M., van Lohuizen, M. et al. (1994). Posterior transformation, neurological abnormalities, and severe hematopoietic defects in mice with a targeted deletion of the *bmi-1* proto-oncogene. *Genes Dev.* **8**, 757-769.
van Lohuizen, M., Verbeek, S., Scheijen, B., Wientjens, E., van der Gulden, H. and Berns, A. (1991). Identification of cooperating oncogenes in *E mu-myc* transgenic mice by provirus tagging. *Cell* **65**, 737-752.
Wang, B. B., Muller-Immergluck, M. M., Austin, J., Robinson, N. T., Chisholm, A. and Kenyon, C. (1993). A homeotic gene cluster patterns the anteroposterior body axis of *C. elegans*. *Cell* **74**, 29-42.
Wang, H., Wang, L., Erdjument-Bromage, H., Vidal, M., Tempst, P., Jones, R. S. and Zhang, Y. (2004a). Role of histone H2A ubiquitination in Polycomb silencing. *Nature* **431**, 873-878.
Wang, L., Brown, J. L., Cao, R., Zhang, Y., Kassis, J. A. and Jones, R. S. (2004b). Hierarchical recruitment of polycomb group silencing complexes. *Mol. Cell* **14**, 637-646.
Wei, J., Zhai, L., Xu, J. and Wang, H. (2006). Role of Bmi1 in H2A ubiquitylation and Hox gene silencing. *J. Biol. Chem.* **281**, 22537-22544.
White, J. G., Southgate, E., Thomson, J. N. and Brenner, S. (1986). The structure of the nervous system of the nematode *Caenorhabditis elegans*. *Philos. Trans. R. Soc. Lond. B Biol. Sci.* **311**, 1-340.

Xu, L., Fong, Y. and Strome, S. (2001a). The *Caenorhabditis elegans* maternal-effect sterile proteins, MES-2, MES-3, and MES-6, are associated in a complex in embryos. *Proc. Natl. Acad. Sci. USA* **98**, 5061-5066.

Xu, L., Paulsen, J., Yoo, Y., Goodwin, E. B. and Strome, S. (2001b). *Caenorhabditis elegans* MES-3 is a target of GLD-1 and functions epigenetically in germline development. *Genetics* **159**, 1007-1017.

Yang, Y., Sun, Y., Luo, X., Zhang, Y., Chen, Y., Tian, E., Lints, R. and Zhang, H. (2007). Polycomb-like genes are necessary for specification of dopaminergic and serotonergic neurons in *Caenorhabditis elegans*. *Proc. Natl. Acad. Sci. USA* **104**, 852-857.

Yu, H., Pretot, R. F., Burglin, T. R. and Sternberg, P. W. (2003). Distinct roles of transcription factors EGL-46 and DAF-19 in specifying the functionality of a polycystin-expressing sensory neuron necessary for *C. elegans* male vulva location behavior. *Development* **130**, 5217-5227.

Zallen, J. A., Yi, B. A. and Bargmann, C. I. (1998). The conserved immunoglobulin superfamily member SAX-3/Robo directs multiple aspects of axon guidance in *C. elegans*. *Cell* **92**, 217-227.

Zhang, H. and Emmons, S. W. (2001). The novel *C. elegans* gene *sop-3* modulates Wnt signaling to regulate Hox gene expression. *Development* **128**, 767-777.

Zhang, H., Azevedo, R. B., Lints, R., Doyle, C., Teng, Y., Haber, D. and Emmons, S. W. (2003). Global regulation of Hox gene expression in *C. elegans* by a SAM domain protein. *Dev. Cell* **4**, 903-915.

Zhang, H., Smolen, G. A., Palmer, R., Christoforou, A., van den Heuvel, S. and Haber, D. A. (2004). SUMO modification is required for in vivo Hox gene regulation by the *Caenorhabditis elegans* Polycomb group protein SOP-2. *Nat. Genet.* **36**, 507-511.

Zhang, T., Sun, Y., Tian, E., Deng, H., Zhang, Y., Luo, X., Cai, Q., Wang, H., Chai, J. and Zhang, H. (2006). RNA-binding proteins SOP-2 and SOR-1 form a novel PcG-like complex in *C. elegans*. *Development* **133**, 1023-1033.

Zhu, P., Zhou, W., Wang, J., Puc, J., Ohgi, K. A., Erdjument-Bromage, H., Tempst, P., Glass, C. K. and Rosenfeld, M. G. (2007). A histone H2A deubiquitinase complex coordinating histone acetylation and H1 dissociation in transcriptional regulation. *Mol. Cell* **27**, 609-621.